# Orbital Surface Hopping with an Electron Thermostat Yields Accurate Dynamics and Detailed Balance

Yong-Tao Ma<sup>†</sup> and Wenjie Dou<sup>\*,†,‡,¶</sup>

†Department of Chemistry, School of Science and Research Center for Industries of the Future, Westlake University, Hangzhou, Zhejiang 310024, China

‡Institute of Natural Sciences, Westlake Institute for Advanced Study, Hangzhou, Zhejiang 310024, China

¶Key Laboratory for Quantum Materials of Zhejiang Province, Department of Physics, School of Science and Research Center for Industries of the Future, Westlake University, Hangzhou,

Zhejiang 310024, China

E-mail: douwenjie@westlake.edu.cn

### **Abstract**

In mixed quantum-classical simulations of molecule-metal surface interactions, the discretization of the metallic electronic continuum typically results in a closed-system representation that fails to capture the open-system nature of the true physical process. This approximation can introduce significant artifacts, including deviations in the dynamical evolution and a violation of the principle of detailed balance. To address this fundamental challenge, we introduce an electronic thermostat into our previously developed orbital surface hopping (OSH) framework, generalizing the method to efficiently handle many discrete electronic states. We first outline the derivation of electronic thermostat orbital surface hopping, where the amplitude of the electronic thermostat is well justified. We then demonstrate that this method can

reproduce accurate dynamics and detailed balance in long time, whereas without electronic thermostat the detailed balance is violated. Thus, this method offers a reliable tool for studying nonadiabatic dynamics near metal surfaces.

### Introduction

Understanding and modeling nonadiabatic effects in surface inelastic scattering and reaction dynamics represent an area of increasing scientific interest. <sup>1–7</sup> These effects are pivotal in governing key processes involving electron and energy transfer at surfaces. <sup>8–10</sup> Accurate simulation of such phenomena requires theoretical frameworks capable of capturing nonadiabatic dynamics. For realistic systems, however, the large number of degrees of freedom renders fully quantum mechanical methods, such as Multi-Configuration Time-Dependent Hartree (MCTDH)<sup>11</sup> and Hierarchical Equations of Motion (HEOM), <sup>12</sup> computationally prohibitive. This computational bottleneck has driven the development of mixed quantum-classical methods as a practical alternative. Among these, the Ehrenfest and surface hopping approaches have gained widespread adoption due to their conceptual clarity and computational efficiency. It is critical to note that, unlike their application in the gas phase, both methods require specific adaptations to accurately capture the unique electronic characteristics of metal surfaces.

In the Electron Friction approach, nuclear motion is classically propagated on the ground-state potential energy surface under the influence of an additional frictional force originating from metal-molecule interactions. <sup>13–22</sup> In contrast, the Classical Master Equation (CME) and Broad-ened Classical Master Equation (BCME) frameworks, <sup>23,24</sup> the electronic degrees of freedom of the metal are treated within an open quantum system framework. In these methods, the electronic states of the metal surface are partially traced out, and electron transfer between the metal and the adsorbate is modeled as stochastic hops between molecular neutral and anionic states—with the latter broadened in the BCME formulation. The metal-molecule interaction is incorporated through a generalized damping term. Notably, the BCME approach has shown remarkable accu-

racy across a broad spectrum of coupling strengths, ranging from the weak to the strong coupling regime. <sup>25</sup> However, a recognized limitation of the BCME method is its restriction to systems with effectively one electronic state, preventing its direct application to problems involving multiple active electronic states. <sup>26</sup>

Perhaps the most prominent method in this category is Independent Electron Surface Hopping (IESH). 27,28 In contrast to the BCME approach, IESH explicitly retains the electronic degrees of freedom of the metal. Within this framework, nuclear dynamics evolve on adiabatic potential energy surfaces constructed by coupling the molecular anionic state with discrete electron states of the metal. Transitions between these surfaces ("hops") are governed by probabilities derived from the time-dependent electronic wavefunctions. The IESH method has accurately reproduced experimental results for NO scattering on the Au(111) surface, <sup>27</sup> showing excellent agreement with measured vibrational energy relaxation and electron population dynamics. Furthermore, the theoretical simulations revealed a steering mechanism that provides additional insight into the scattering process. The conceptual foundation of IESH is closely related to the trajectory surfacehopping time-dependent Kohn-Sham (TDKS) approach pioneered by Prezhdo and coworkers. <sup>29,30</sup> This lineage has inspired the development of several popular software packages, such as PYX-AID, <sup>31</sup> Hefei-NAMD <sup>32</sup> and GTSH, <sup>33</sup> which are designed for simulating nonadiabatic molecular dynamics in condensed matter systems. In our recent work, we theoretically demonstrated that, within the independent electron approximation, the hopping probabilities can be formulated directly in terms of orbital densities involved in each hopping event.<sup>34</sup> This formulation, which we term the Orbital Surface Hopping (OSH) method, offers a more physically transparent picture by tracking electron evolution through individual orbitals at the metal surface. The OSH approach achieves accuracy comparable to IESH but at a substantially reduced computational cost.

A fundamental limitation of the original IESH and OSH methods lies in their discretization of the electronic continuum, which enforces a closed-system representation. This approximation severs the essential energy dissipation pathway into the metal surface, resulting in spurious conservation of the total energy. Such behavior is unphysical given the vast heat capacity of a metal and

introduces artifacts including erroneous long-time dynamics and a violation of detailed balance. While enlarging the basis set of discrete states could better approximate the continuum, it does so at a prohibitive computational cost. This inherent shortcoming was recognized by the Tully group three years after IESH was first introduced, prompting them to propose an electronic thermostat methodology. <sup>35</sup> The approach was motivated by two physical insights: first, that electron–electron scattering occurs on a much shorter timescale than nuclear motion, and second, that the probabilities for transferring a high-energy electron to a low-energy hole should obey a Boltzmann distribution. Implemented in a Monte Carlo framework, this thermostat successfully recovers correct equilibrium populations and kinetic energy. <sup>25</sup> Despite its conceptual importance, the method initially received limited attention. Only recently has its utility been demonstrated in other contexts: the Prezhdo group employed it in an Auger process to enforce electron number conservation, <sup>36</sup> and the Jiang group used it in initial electron states sampling for NO scattering on Au(111). <sup>37</sup> Building on these developments and grounded in open quantum system theory combined with the concept of orbital densities, we have formulated a new electronic thermostat strategy. This methodology is implemented in our OSH approach. We benchmark its performance against both the Tully's electronic thermostat and the reference HEOM method. Results indicate that our proposed electron thermostat significantly improves the approach to equilibrium electronic populations and yields more physically accurate kinetic energy distributions.

This paper is organized as follows. Section II details the computational methodology. The results and corresponding discussion are presented in Section III. Finally, Section IV provides the concluding remarks.

# Methodology

In general, we define the Hamiltonian for a non-interacting system coupled to a continuous bath as:

$$\hat{H}_{total} = \hat{H}_s + \hat{H}_b + \hat{H}_c, \tag{1}$$

in which, the system Hamiltonian is:

$$\hat{H}_s = \sum_{mn} h_{mn}(\hat{R}) \hat{d}_m^{\dagger} \hat{d}_n + U(\hat{R}) + T(\hat{P}). \tag{2}$$

The continuous bath Hamiltonian and the system-bath coupling Hamiltonian are as follows.

$$\hat{H}_b = \int dk' \, \varepsilon_{k'} \hat{c}_{k'}^{\dagger} \hat{c}_{k'}, \tag{3}$$

$$\hat{H}_{c} = \sum_{m} \int dk' \left( V_{mk'}(\hat{R}) \hat{d}_{m}^{\dagger} \hat{c}_{k'} + V_{mk'}^{*}(\hat{R}) \hat{c}_{k'}^{\dagger} \hat{d}_{m} \right). \tag{4}$$

Our approach begins by discretizing the continuous electronic spectrum of the metal surface, a common first step in IESH and OSH simulations. To incorporate the electrostatic interactions neglected by this discretization, we reformulate the problem within an open quantum system framework. Here, the "system" comprises the adsorbate, the discretized metal surface, and their interaction, while the "bath" is composed of the remaining continuum of electronic states. Formally, the bath Hamiltonian is  $\hat{H}_b = \int dk' \, \epsilon_{k'} c_{k'}^{\dagger} c_{k'}$ , where the integration excludes the discretized wavevectors  $(k' \notin k)$ . However, in our numerical implementation, the bath is itself represented by a limited number of discrete levels. This practical approximation should not impact our qualitative findings; therefore, for the sake of a general discussion, we do not enforce the strict continuum limit for the bath. For the system-bath coupling, we assume that the molecule-surface interaction is already contained within the system Hamiltonian through the discretization method, following the work of Tully et al.  $^{25,28,38}$ 

As previously noted, the finite number of discrete energy levels is much smaller than the original continuum, leading to a small mean energy level spacing  $\Delta E$ . This spacing is significantly less than the hybridization width  $\Gamma$  ( $\Delta E < \Gamma$ ). Consequently, the timescales for electronic dissipation in the bath ( $\tau_b$ ) and system electron transfer ( $\tau_s$ ) are well separated, with dissipation being orders of magnitude faster (i.e.,  $\tau_b \ll \tau_s$ ). This clear separation of timescales makes it reasonable to treat the system-bath interaction within the weak coupling framework. Under the Born-Markovian

approximation, the evolution of density matrix can be described as:

$$\dot{\hat{\rho}}_s = -\frac{i}{\hbar}[\hat{H}_s, \hat{\rho}_s] + \hat{\hat{L}}_{bs}\hat{\rho}_s. \tag{5}$$

The  $\hat{\hat{L}}_{bs}$  is the Liouvelle superoperator. It opetrate on the  $\hat{
ho}_s$  can be given as

$$\hat{\hat{L}}_{bs}\hat{\boldsymbol{\rho}}_{s} = \frac{1}{\hbar^{2}} \int_{0}^{\infty} d\tau e^{-i\hat{H}t/\hbar} tr_{b}([\hat{H}_{c}(t), [\hat{H}_{c}(t-\tau), e^{i\hat{H}t/\hbar}\hat{\boldsymbol{\rho}}_{s}(t)e^{-i\hat{H}t/\hbar} \bigotimes \hat{\boldsymbol{\rho}}_{b}^{eq}]]) e^{i\hat{H}t/\hbar}, \tag{6}$$

which is a "Redfield equation" in Schrodinger picture.

The evolution of the single-particle reduced density matrix element, defined as  $\hat{\sigma}_{jk} = \text{tr}_e \hat{\rho}_s \hat{d}_j^{\dagger} \hat{d}_k$ , is derived by right-multiplying Eq.(5) with the operator  $\hat{d}_j^{\dagger} \hat{d}_k$  and subsequently performing the trace over the entire electronic Hilbert space.

$$\dot{\hat{\sigma}}_s = -\frac{\mathrm{i}}{\hbar} \left[ \hat{H}_{\text{total}}^{orb}, \hat{\sigma}_s \right] + \text{tr}_e(\hat{\hat{L}}_{bs} \hat{\rho}_s \hat{d}_j^{\dagger} \hat{d}_k). \tag{7}$$

The first two terms in Eq. 7 are consistent with our established results (Ref. 34). However, the derivation of the final term is more involved. It can be rigorously derived by direct application of Wick's theorem. <sup>39,40</sup> Here, we follow the treatment presented in Ref. 39. Finally, the evolution of the orbital density matrix in the adiabatic representation is governed by:

$$\dot{\hat{\sigma}}_s = -\frac{\mathrm{i}}{\hbar} \left[ \hat{H}_{\text{total}}^{orb}, \hat{\sigma}_s \right] - \frac{1}{2\hbar} [\hat{\Gamma}, \hat{\sigma}_s]_+ + \frac{1}{2\hbar} [f(\hat{h}), \hat{\sigma}_s]_+. \tag{8}$$

Here f is the Fermi distribution functions  $f(\varepsilon)=1/[e^{(\varepsilon-\mu_b)/k_BT}+1]$  and  $\hat{H}^{orb}_{total}$  represents the total Hamiltonian in the single-body basis set  $\{|j\rangle,j=1,\ldots,m\}$ :

$$\hat{H}_{\text{total}}^{orb} = \hat{T}_{\text{n}} + U(\hat{R}) + \sum_{jk}^{m} h_{jk}(R) |j\rangle\langle k|, \qquad (9)$$

 $U(\mathbf{R})$  represents the pure nuclear potential energy.

This equation can be addressed within a quasi-classical framework. To this end, we perform a partial Wigner transformation of Eq. 8 over the nuclear degrees of freedom. The resulting equation comprises two distinct contributions: 1. The second term constitutes the core of the orbital quantum-classical Liouville equation (o-QCLE). For this term, we retain the Wigner-Moyal expansion to first order in the nuclear momenta, consistent with the standard approach. 41 2. The final term represents electronic dissipation at the metal surface, which occurs on a timescale much shorter than nuclear motion. This timescale separation justifies the application of the Condon approximation, allowing us to truncate the corresponding Wigner-Moyal operator to its zero-th order. 39,40,42 Applying these approximations yields the final working equation:

$$\frac{\partial \hat{\sigma}_{W}^{jk}(\boldsymbol{R},\boldsymbol{P},t)}{\partial t} = -i\omega^{jk}\sigma_{W}^{jk}(\boldsymbol{R},\boldsymbol{P},t) + \sum_{l}\sum_{a}\frac{P_{a}}{M_{a}}(\sigma_{W}^{jl}d_{lk}^{a} - d_{jl}^{a}\sigma_{W}^{lk}) 
- \sum_{a}\frac{P_{a}}{M_{a}}\frac{\partial \sigma_{W}^{jk}}{\partial R_{a}} - \frac{1}{2}\sum_{l}\sum_{a}\left(F_{a}^{jl}\frac{\partial \sigma_{W}^{lk}}{\partial R_{a}} + \frac{\partial \sigma_{W}^{jl}}{\partial P_{a}}F_{a}^{lk}\right) + \sum_{a}\frac{\partial U}{\partial R_{a}}\frac{\partial \sigma_{W}^{jk}}{\partial P_{a}} 
- \frac{1}{2}\sum_{l}(\Gamma_{jl}\sigma_{W}^{lk} + \sigma_{W}^{jl}\Gamma_{lk}) + \frac{1}{2}(f(h_{jj})\Gamma_{jk} + \Gamma_{jk}f(h_{kk})), \tag{10}$$

where  $\omega^{jk} = (\varepsilon_j - \varepsilon_k)/\hbar$ . The nonadiabatic coupling matrix elements and the force calculated under Hellman Feynman equation are given as:

$$d_{jk}^{a} = \left\langle \phi_{j}(\mathbf{R}) \middle| \frac{\partial}{\partial R_{a}} \middle| \phi_{k}(\mathbf{R}) \right\rangle = -\frac{F_{a}^{jk}}{\hbar \omega^{jk}},\tag{11}$$

$$F_a^{jk} = \langle \phi_i(\mathbf{R}) | [\partial h / \partial R_a] | \phi_k(\mathbf{R}) \rangle. \tag{12}$$

To implement the surface hopping approach, the nuclei freedom  $\mathbf{R}$ ,  $\mathbf{P}$  propagate by the Hamilton equations of motion:

$$\dot{R} = \frac{P}{M},\tag{13}$$

$$\dot{\mathbf{P}} = -\frac{\partial U}{\partial \mathbf{R}} + \sum_{i=1}^{n} \mathbf{F}_{\lambda_i, \lambda_i}.$$
 (14)

The nuclei evolve subject to the single-particle forces derived from the occupied orbitals, rather than on a single potential energy surface of an active state. Concurrently, the electronic subsystem is propagated according to the equation of motion for the single-particle density matrix.

$$\dot{\sigma}_{ij}(t) = -i\omega^{ij}\sigma_{ij}(t) - \frac{P}{M} \cdot \sum_{k} (d_{ik}\sigma_{kj} - \sigma_{ik}d_{kj})$$

$$-\frac{1}{2}\sum_{l} (\Gamma_{il}\sigma_{lj} + \sigma_{jl}\Gamma_{li}) + \frac{1}{2}(f(h_{ii})\Gamma_{ij} + \Gamma_{ij}f(h_{jj})).$$
(15)

The probability of hopping from the orbital  $\lambda_i$  to the orbital j is

$$g_{j \leftarrow \lambda_i} = \begin{cases} \max \left\{ -2\operatorname{Re}(\sigma_{j\lambda_i}^* \dot{\mathbf{R}} \cdot \mathbf{d}_{j\lambda_i}) \Delta t' / \sigma_{\lambda_i \lambda_i}, 0 \right\} & j \notin \vec{\lambda} \\ 0 & j \in \vec{\lambda} \end{cases} . \tag{16}$$

The stochastic hopping algorithm is identical to that of FSSH,<sup>43</sup> albeit hopping will be considered for each occupied electron. To minimize hopping, no more than one electron is allowed to transition to a different orbital per nuclear propagating time step.

The second hopping mechanism originates from the rapid electronic dissipation within the metal surface. Since the continuous bath degrees of freedom have been traced out, its influence is captured implicitly. This fast dissipation justifies the use of the secular approximation, wherein we retain only the diagonal elements of the single-particle density matrix  $\sigma$ . Consequently, neglecting nuclear dynamics and hopping events induced by direct non-adiabatic (derivative) coupling, Eq. 15 becomes the simplified form:

$$\dot{\sigma}_{ii} = -\Gamma_{ii}(\sigma_{ii} - f(h_{ii})). \tag{17}$$

Our derivation of the hopping probability follows an occupation number formalism, where each orbital is either occupied (1) or unoccupied (0), analogous to the treatment in Ref. 44. The specific probability for a hop to occur involving orbital i is:

$$g_{i'\leftarrow i} = \begin{cases} \max\{\Gamma_{ii}(1 - f(h_{ii})), 0\} & (i' \in 0, i \in 1) \\ \max\{\Gamma_{ii}f(h_{ii}), 0\} & (i' \in 1, i \in 0) \end{cases}$$
 (18)

This hopping probability is governed by the hybridization function,  $\Gamma_{ii}$ , which quantifies the spectral broadening and dictates the inverse lifetime of the electronic state. Our model employs the wide-band and Condon approximations, justified by the separation of timescales between rapid electronic dissipation at the metal surface and slower nuclear motion. This allows  $\Gamma_{ii}$  to be treated as an energy-independent constant. We assign it a value comparable to the characteristic energy scale of the problem—specifically, the level spacing near the Fermi energy, where electronic excitations are dominant.

For comparative analysis, we have implemented Tully's electronic thermostat method <sup>35</sup> within our OSH framework. In this approach, electron dynamics are propagated using the first three terms of Eq. 15. The second hopping mechanism is replaced by a stochastic process: an occupied orbital i and an unoccupied orbital j are randomly selected. A hopping event from i to j is then accepted with a probability: min(1,  $e^{-(h_{jj}-h_{ii})/k_BT}$ ). This entire procedure is triggered at each time step with a probability of  $\Delta t/\tau$ , where  $\tau$  is the characteristic timescale of the thermostat. A comprehensive discussion and comparison of the results are presented subsequently.

### **Results and discussion**

To test our new electron thermostat method, we employ the Newns-Anderson model, which has been successfully applied to study non-adiabatic effects at gas-metal interfaces. <sup>25,27,28,45,46</sup> To validate the accuracy of our method, we used the highly accurate but computationally expensive Hierarchical Equations of Motion (HEOM) method <sup>47</sup> as a benchmark. To make these benchmark calculations feasible, minor adjustments to the system parameters were necessary. For larger systems where HEOM becomes prohibitively expensive, our comparison is confined to assessing the performance of our OSH method with and without the electronic thermostat.

### **Simulation details**

The Newns-Anderson Hamiltonian with one impurity molecule orbital and a continuum of metal electron orbitals that discretized into M orbitals is given as:

$$\hat{H}_{el}(\mathbf{R}) = U_0(\mathbf{R}) + (U_1(\mathbf{R}) - U_0(\mathbf{R}))c_a^{\dagger}c_a + \sum_{n=1}^{M} \varepsilon_n c_n^{\dagger}c_n + \sum_{n=1}^{M} (V_n(\mathbf{R})c_a^{\dagger}c_n + V_n(\mathbf{R})^*c_n^{\dagger}c_a),$$
(19)

where  $c_{\varepsilon}^{\dagger}(c_{\varepsilon})$  and  $c_{a}^{\dagger}(c_{a})$  are the fermionic creation (annihilation) operators of metal and molecule orbital, respectively.  $V(\mathbf{R})$  are the couplings between molecular and metal orbitals.  $U_{1}(\mathbf{R}), U_{0}(\mathbf{R})$  are the potential energy surfaces of the anionic and neutral molecule, respectively. We consider a 1D double well potential following Refs.  $^{25,38,45,46}$ 

$$U_0(R) = \frac{1}{2}M\omega^2 R^2, (20)$$

$$U_1(R) - U_0(R) = -M\omega^2 gR + \frac{1}{2}M\omega^2 g^2 + \Delta G.$$
 (21)

Here, the displacement parameter g is related to reorganization energy by  $E_{\rm r}=\frac{1}{2}M\omega^2g^2$ . The parameters used for our model are (units: a.u.)  ${\rm m}=2.0\times10^3,~\omega=2.0\times10^{-4},~g=20.6097,$   $\Delta G_0=-3.8\times10^{-3}$  and  $kT=9.5\times10^{-4}$ . These parameters are prepared according to Ref. 25,45. The wide-band spectral density function is used and the hybridization function,

$$\Gamma(\varepsilon; \mathbf{R}) \equiv 2\pi \sum_{k} |V(\varepsilon, \mathbf{R})|^2 \delta(\varepsilon - \varepsilon_k),$$
 (22)

is assumed to be a constant  $\Gamma$  across the interval  $E_- = -W/2 + \mu$  and  $E_+ = W/2 + \mu$ . Here, W and  $\mu$  are the bandwidth and the chemical potential, respectively. The trapezoid discretization procedure is adopted following Ref. 25, as it is reported to be numerically more stable <sup>25</sup> and equally accurate as Gauss-Legendre procedure for small bandwidths. Throughout this section, the occu-

pation of the metal orbitals are prepared at "zero temperature", i.e., all the diabatic orbitals below Fermi level  $\mu$  are occupied. The impurity molecular orbital, on the other hand, is unoccupied.

To evaluate the performance of electron thermostat, we initialized an ensemble of trajectories from the Boltzmann distribution of  $U_0$ , imparting additional initial kinetic energy. <sup>25,48</sup> The dynamics were compared under two scenarios: (1) with only the electronic thermostat, and (2) with the electronic thermostat plus an external nuclear friction force. This friction, parameterized universally by  $\gamma_{\text{ext}} = 2\omega$ , models the contribution from phononic energy dissipation into the surface.

### **Benchmarked with HEOM methods**

The simulated time-dependent kinetic energy and impurity hole population are compared in Fig. 1 across three methods: HEOM (benchmark), OSH, and OSH with electron thermostat (labeled OSH-ETS). All HEOM simulations were performed with the HierarchicalEOM.jl package.  $^{49,50}$  The HierarchicalEOM.jl software package provides a user-friendly and efficient tool for simulating complex open quantum systems, including non-Markovian effects due to non-perturbative interaction with one, or multiple, environments. The initial total energy was set to 2kT, resulting in an initial kinetic energy of kT. A displacement parameter of g = 15.7706 was used to enhance computational efficiency. In our simulations, the hybridization function is represented by a Lorentzian form with  $\Gamma = 6.4 \times 10^{-4}$ . The Fermi energy is set to zero. The Fermi distribution is approximated using a Padé expansion, and the HEOM method is executed with 4 exponential terms and a hierarchy tier of 4 to ensure converged results. The electronic bandwidth is set to  $W = 6.4 \times 10^{-3}$ , and the continuum is represented by 40 discrete electron levels.

As shown in Fig. 1, the OSH method with our electronic thermostat (OSH-ETS) successfully drives both the population and kinetic energy to converge with the HEOM benchmark results at long times. In contrast, while the standard OSH method (without a thermostat) reaches an equilibrium more rapidly, this equilibrium state exhibits a significant discrepancy from the HEOM result. A detailed examination of the dynamics reveals that OSH and OSH-ETS yield similar trajectories for the first 20  $\omega t$ . Beyond this point, the electronic thermostat in OSH-ETS becomes active, guid-

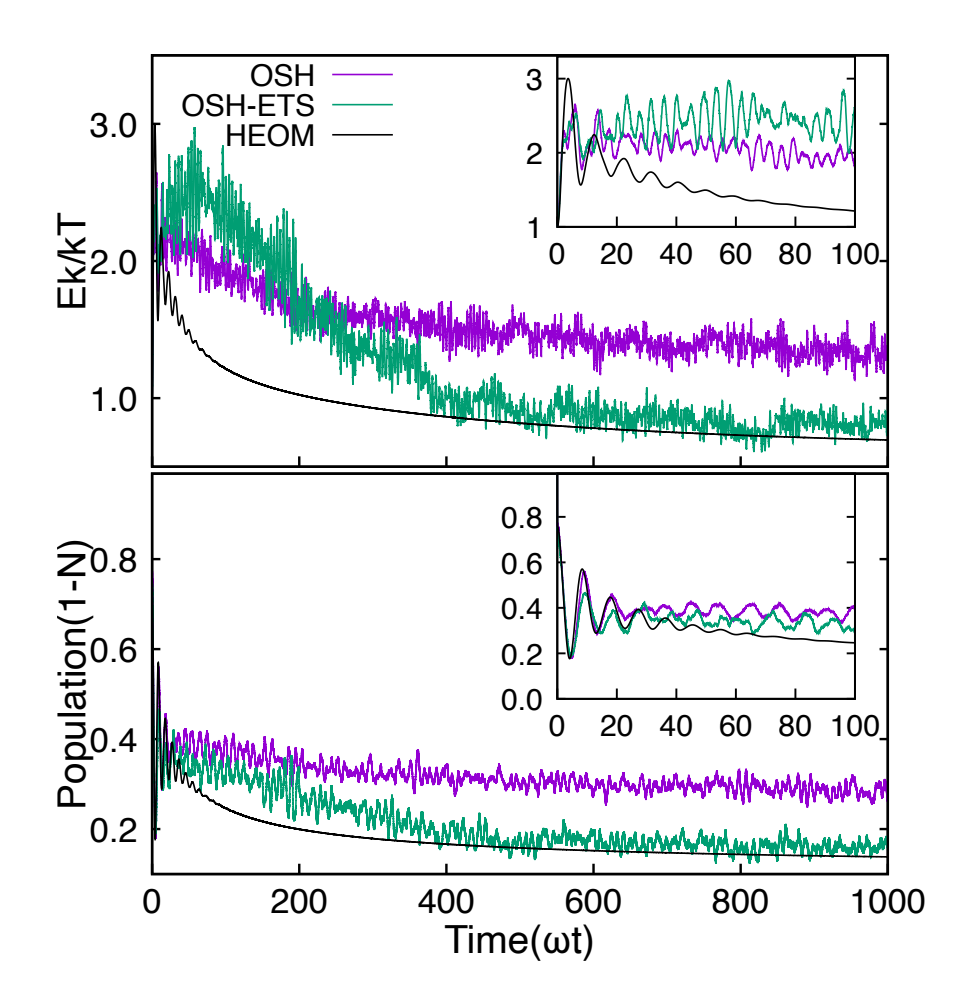


Figure 1: Time evolution of the impurity hole population and kinetic energy, comparing the standard OSH, OSH with electronic thermostat (OSH-ETS), and HEOM methods. The inset shows the short-time evolution of the same quantities.

ing the impurity hole population and kinetic energy toward the correct thermal equilibrium. This successful reproduction of the benchmark dynamics demonstrates the accuracy and utility of our new electronic thermostat method.

### Comparison under pure electron thermostat

To evaluate the performance of our new thermostat method, we simulated a wide range of molecule-metal coupling strengths (Fig. 2). We use the bandwidth W and number of states M from Ref. 25, where convergence of the IESH method was demonstrated. Since our previous work established that OSH converges at least as fast as IESH with respect to the state number at a fixed W, <sup>34</sup> we retain these parameters for all calculations.

The results demonstrate that only the methods incorporating an electronic thermostat—both our OSH-ETS and Tully's approach (labled OSH- $\tau$  = 100)—faithfully reproduce the correct equilibrium kinetic energy and impurity hole population. In contrast, the standard OSH method without a thermostat shows significant deviations in the impurity population across different coupling regimes, underscoring the critical role of the electronic dissipation channel. The simulations lead to two principal conclusions: Essential Role of Electronic Thermostat: Accurate equilibrium kinetic energy and impurity population are only achieved when an electronic thermostat (either OSH-ETS or Tully's method) is employed. Failure of Standard OSH: The standard OSH method, lacking this dissipation mechanism, gives rise to significant errors in the impurity population that persist across different coupling strengths.

### Comparison with external friction

Figure 3 displays the impurity hole population dynamics in the presence of external nuclear friction across various coupling strengths. A key observation is that the inclusion of nuclear friction drives all methods toward a similar equilibrium population, with the electronic thermostats primarily serving to accelerate the equilibration process. In most cases, our method and Tully's yield nearly identical results. A significant deviation, however, occurs at the specific coupling strength

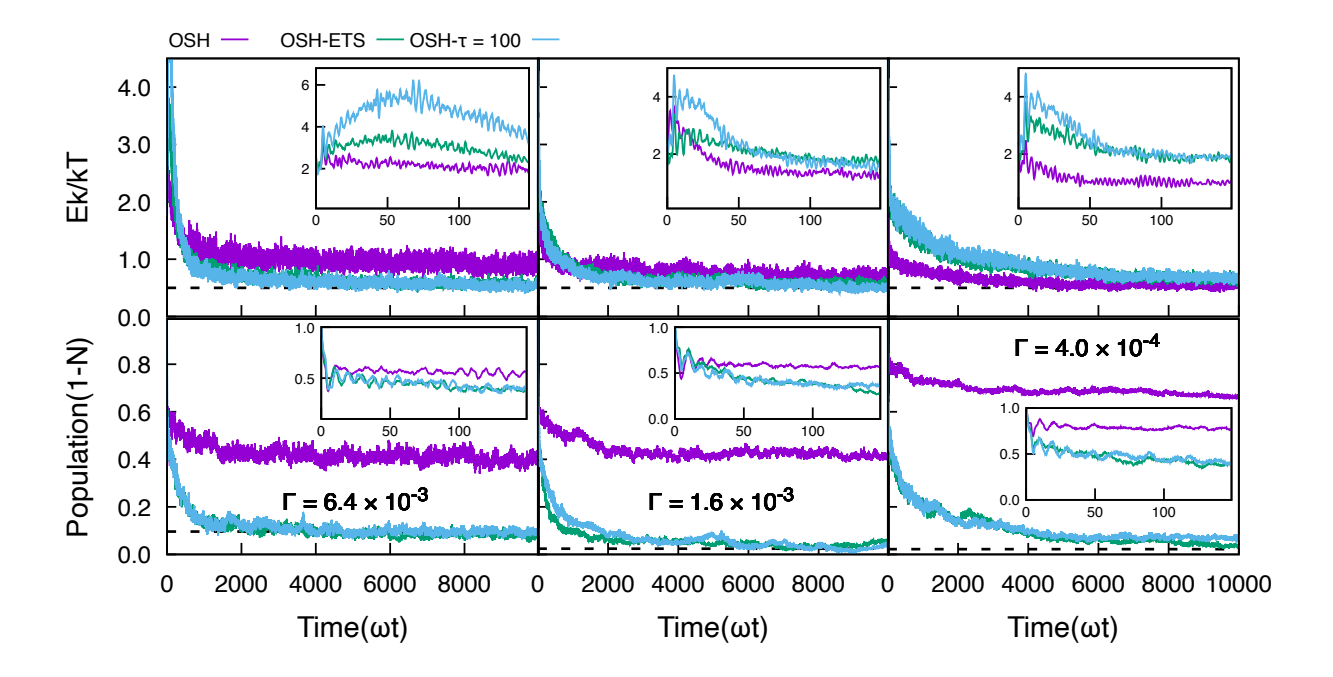


Figure 2: Kinetic energy (top) and impurity hole population dynamics (bottom) as a function of time. Results are shown for three methods: OSH, OSH-ETS, and OSH with Tully's electronic thermostat approach ( $\tau$  = 100), across a range of coupling strengths: (left)  $\Gamma$  = 6.4 × 10<sup>-3</sup>, (middle)  $\Gamma$  = 1.6 × 10<sup>-3</sup>, and (right)  $\Gamma$  = 4.0 × 10<sup>-4</sup>. The insets zoom in on the short-time behavior.

of  $\Gamma=6.4\times10^{-3}$ . At this value, Tully's method produces a result similar to the case without any electronic thermostat, whereas our OSH-ETS method maintains an accurate population. To verify the robustness of our finding, we conducted additional simulations at this coupling with different friction coefficients  $\gamma$  (see Figure S1, Appendix). These tests confirm that while varying  $\gamma$  alters the kinetic rates, it does not affect the long-time population limit. Under this specific condition, our method integrated with the OSH framework provides a more accurate result than Tully's. For Tully's method, the outcome was found to be largely insensitive to the value of the thermostat timescale  $\tau$ .

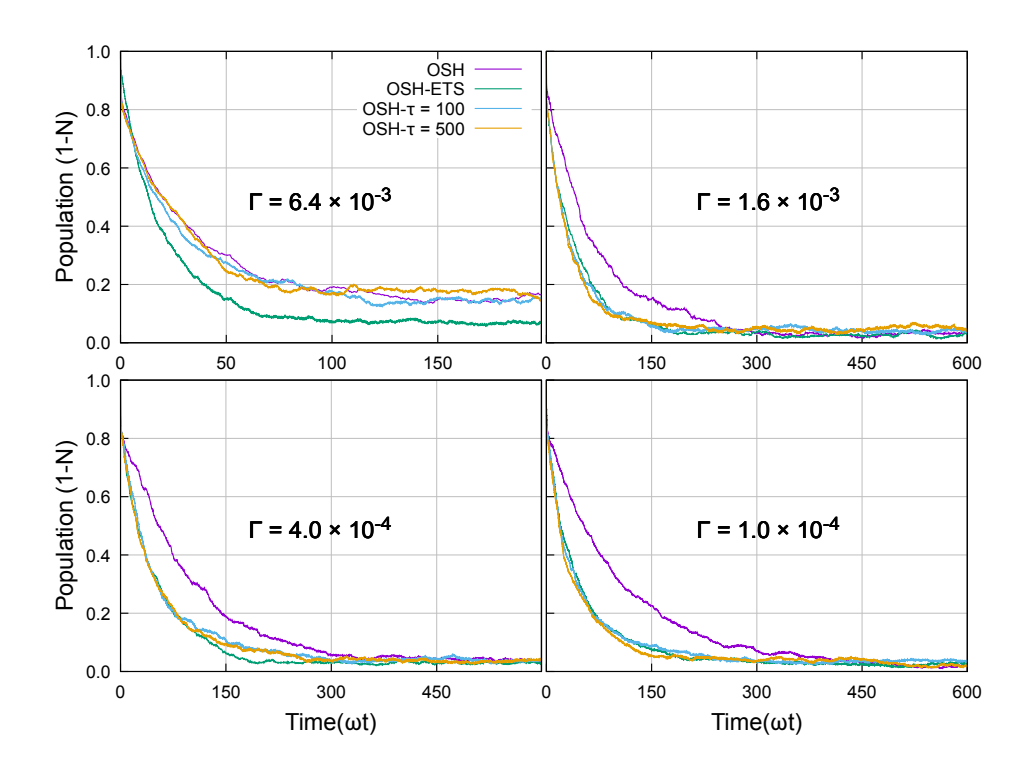


Figure 3: Impurity hole population dynamics as a function of time for OSH, OSH-ETS and OSH ( $\tau = 100$  and 500 for Tully's electronic thermostat method).

### **Conclusion**

In summary, we have developed a novel electronic thermostat method to model energy dissipation into a continuum of surface states. This approach is grounded in open quantum system theory and

seamlessly integrates with our previously established OSH framework. The method was rigorously validated against the numerically exact HEOM approach, demonstrating that OSH with our thermostat correctly drives the system toward the accurate equilibrium kinetic energy and population.

Extensive comparisons across a broad parameter range reveal that, in the presence of a pure electronic thermostat, both our method and Tully's achieve accurate equilibrium states. When external nuclear friction is included, the performance of our method is largely comparable to Tully's electron thermostat method.

Our analysis demonstrates that both our method and Tully's electronic thermostat are capable and efficient for simulating metal surfaces, delivering comparable results. The choice between them can be guided by the specific problem: Tully's method, which conserves electron number, remains a robust option for closed systems like Auger recombination. Our method, derived from open system theory, offers a complementary and formally rigorous pathway for handling energy dissipation, integrating seamlessly with our broader OSH framework.

## Acknowledgement

W. D. thanked the funding from the National Natural Science Foundation of China (no. 22361142829) and Zhejiang Provincial Natural Science Foundation (no. XHD24B0301)). Y.-T. Ma thanked the project (Grant No. ZR2021MB081) supported by Shandong Provincial Natural Science Foundation and thanked Dr. Yu Wang and Mr. Ruihao Bi for helpful discussion. The authors thanked the Westlake University Supercomputer Center for facility support and technical assistance.

# Compare parameters for external fiction

At a coupling strength of  $\Gamma = 6.4 \times 10^{-3}$ , our electron thermostat method shows a marked deviation from Tully's result (Fig. 3). To establish robustness, we systematically varied the friction coefficient  $\gamma$  at this coupling. As shown in Fig. S1, while  $\gamma$  modulates the transient kinetics, it does not affect the steady-state population. This finding underscores that, under this specific con-

ditions, our OSH-electron thermostat method achieves a more physically accurate representation than Tully's.

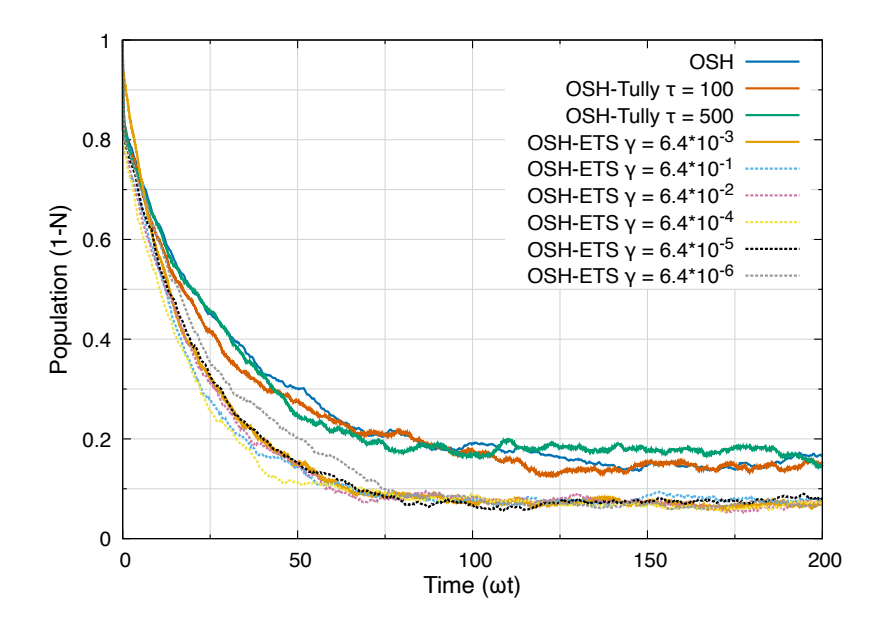


Figure 4: Impurity hole population dynamics and kinetic energy as a function of time for OSH, OSH-ETS and OSH with Tully's electronic thermostat approach ( $\tau = 100$  and 500).

### References

- (1) Meng, G.; Gardner, J.; Hertl, N.; Dou, W.; Maurer, R. J.; Jiang, B. First-Principles Nonadia-batic Dynamics of Molecules at Metal Surfaces with Vibrationally Coupled Electron Transfer. Phys. Rev. Lett. 2024, 133, 036203.
- (2) Wu, Q.; Zhou, L.; Schatz, G. C.; Zhang, Y.; Guo, H. Mechanistic Insights into Photocatalyzed H2 Dissociation on Au Clusters. <u>Journal of the American Chemical Society</u> **2020**, <u>142</u>, 13090–13101, PMID: 32615759.
- (3) Huang, Y.; Rettner, C. T.; Auerbach, D. J.; Wodtke, A. M. Vibrational Promotion of Electron Transfer. Science **2000**, 290, 111–114.

- (4) Rahinov, I.; Kandratsenka, A.; Schäfer, T.; Shirhatti, P.; Golibrzuch, K.; Wodtke, A. M. Vibrational energy transfer in collisions of molecules with metal surfaces. <a href="https://phys.chem.chem.">Phys. 2024, 26, 15090–15114.</a>
- (5) Reilly, C. S.; Auerbach, D. J.; Zhang, L.; Guo, H.; Beck, R. D. Quantum interference observed in state-resolved molecule-surface scattering. Science **2025**, 387, 962–967.
- (6) Zhang, S.; Liu, Z.; Bao, P.; Shi, Q. A multiset matrix product state approach to hierarchical equations of motion and its application to vibrational relaxation on metal surfaces. <u>The</u> Journal of Chemical Physics **2025**, 163, 094102.
- (7) Preston, R. J.; Ke, Y.; Rudge, S. L.; Hertl, N.; Borrelli, R.; Maurer, R. J.; Thoss, M. Nonadia-batic Quantum Dynamics of Molecules Scattering from Metal Surfaces. <u>Journal of Chemical</u> Theory and Computation **2025**, 21, 1054–1063, PMID: 39873222.
- (8) Tully, J. C. Chemical Dynamics at Metal Surfaces. <u>Annual Review of Physical Chemistry</u> **2000**, 51, 153–178.
- (9) Auerbach, D. J.; Tully, J. C.; Wodtke, A. M. Chemical dynamics from the gas-phase to surfaces. Natural Sciences **2021**, 1, e10005.
- (10) Alec M. Wodtke \*, J. C. T.; Auerbach, D. J. Electronically non-adiabatic interactions of molecules at metal surfaces: Can we trust the Born–Oppenheimer approximation for surface chemistry? International Reviews in Physical Chemistry 2004, 23, 513–539.
- (11) Beck, M.; Jäckle, A.; Worth, G.; Meyer, H.-D. The multiconfiguration time-dependent Hartree (MCTDH) method: a highly efficient algorithm for propagating wavepackets. <a href="Physics 2000">Physics 2000</a>, <a href="324">324</a>, 1–105.
- (12) Xu, M.; Liu, Y.; Song, K.; Shi, Q. A non-perturbative approach to simulate heterogeneous electron transfer dynamics: Effective mode treatment of the continuum electronic states. <u>The</u> Journal of Chemical Physics **2019**, 150, 044109.

- (13) Dou, W.; Miao, G.; Subotnik, J. E. Born-Oppenheimer Dynamics, Electronic Friction, and the Inclusion of Electron-Electron Interactions. Phys. Rev. Lett. **2017**, 119, 046001.
- (14) Smith, B. B.; Hynes, J. T. Electronic friction and electron transfer rates at metallic electrodes. The Journal of Chemical Physics **1993**, 99, 6517–6530.
- (15) d'Agliano, E. G.; Kumar, P.; Schaich, W.; Suhl, H. Brownian motion model of the interactions between chemical species and metallic electrons: Bootstrap derivation and parameter evaluation. Phys. Rev. B **1975**, 11, 2122–2143.
- (16) Brandbyge, M.; Hedegård, P.; Heinz, T. F.; Misewich, J. A.; Newns, D. M. Electronically driven adsorbate excitation mechanism in femtosecond-pulse laser desorption. <a href="https://example.com/Phys. Rev. B">Phys. Rev. B</a> 1995, 52, 6042–6056.
- (17) Head-Gordon, M.; Tully, J. C. Molecular dynamics with electronic frictions. <u>The Journal of</u> Chemical Physics **1995**, 103, 10137–10145.
- (18) Dou, W.; Nitzan, A.; Subotnik, J. E. Frictional effects near a metal surface. <u>The Journal of Chemical Physics</u> **2015**, 143, 054103.
- (19) Dou, W.; Subotnik, J. E. A many-body states picture of electronic friction: The case of multiple orbitals and multiple electronic states. <u>The Journal of Chemical Physics</u> **2016**, <u>145</u>, 054102.
- (20) Bode, N.; Kusminskiy, S. V.; Egger, R.; von Oppen, F. Scattering Theory of Current-Induced Forces in Mesoscopic Systems. Phys. Rev. Lett. **2011**, 107, 036804.
- (21) Lü, J.-T.; Brandbyge, M.; Hedegård, P.; Todorov, T. N.; Dundas, D. Current-induced atomic dynamics, instabilities, and Raman signals: Quasiclassical Langevin equation approach. Phys. Rev. B **2012**, 85, 245444.
- (22) Persson, B.; Persson, M. Vibrational lifetime for CO adsorbed on Cu(100). <u>Solid State</u> Communications **1980**, 36, 175–179.

- (23) Dou, W.; Nitzan, A.; Subotnik, J. E. Surface hopping with a manifold of electronic states. II. Application to the many-body Anderson-Holstein model. <u>The Journal of Chemical Physics</u> 2015, 142, 084110.
- (24) Dou, W.; Nitzan, A.; Subotnik, J. E. Surface hopping with a manifold of electronic states. III. Transients, broadening, and the Marcus picture. <u>The Journal of Chemical Physics</u> **2015**, <u>142</u>, 234106.
- (25) Miao, G.; Ouyang, W.; Subotnik, J. A comparison of surface hopping approaches for capturing metal-molecule electron transfer: A broadened classical master equation versus independent electron surface hopping. The Journal of Chemical Physics 2018, 150, 041711.
- (26) Dou, W.; Subotnik, J. E. Nonadiabatic Molecular Dynamics at Metal Surfaces. <u>The Journal</u> of Physical Chemistry A **2020**, 124, 757–771, PMID: 31916769.
- (27) Shenvi, N.; Roy, S.; Tully, J. C. Dynamical Steering and Electronic Excitation in NO Scattering from a Gold Surface. Science **2009**, 326, 829–832.
- (28) Shenvi, N.; Roy, S.; Tully, J. C. Nonadiabatic dynamics at metal surfaces: Independent-electron surface hopping. The Journal of Chemical Physics **2009**, 130, 174107.
- (29) Craig, C. F.; Duncan, W. R.; Prezhdo, O. V. Trajectory Surface Hopping in the Time-Dependent Kohn-Sham Approach for Electron-Nuclear Dynamics. <a href="Phys. Rev. Lett.">Phys. Rev. Lett.</a> **2005**, 95, 163001.
- (30) Habenicht, B. F.; Craig, C. F.; Prezhdo, O. V. Time-Domain Ab Initio Simulation of Electron and Hole Relaxation Dynamics in a Single-Wall Semiconducting Carbon Nanotube. <a href="https://pxx.ncbi.nlm.ncbi.
- (31) Akimov, A. V.; Prezhdo, O. V. The PYXAID Program for Non-Adiabatic Molecular Dynamics in Condensed Matter Systems. <u>Journal of Chemical Theory and Computation</u> **2013**, <u>9</u>, 4959–4972, PMID: 26583414.

- (32) Zheng, Q.; Chu, W.; Zhao, C.; Zhang, L.; Guo, H.; Wang, Y.; Jiang, X.; Zhao, J. Ab initio nonadiabatic molecular dynamics investigations on the excited carriers in condensed matter systems. WIREs Computational Molecular Science **2019**, 9, e1411.
- (33) Liu, X.-Y.; Chen, W.-K.; Fang, W.-H.; Cui, G. Nonadiabatic Dynamics Simulations for Photoinduced Processes in Molecules and Semiconductors: Methodologies and Applications. Journal of Chemical Theory and Computation **2023**, 19, 8491–8522, PMID: 37984502.
- (34) Ma, Y.-T.; Bi, R.-H.; Dou, W. Orbital Surface Hopping from the Orbital Quantum-Classical Liouville Equation for Nonadiabatic Dynamics of Many-Electron Systems. <u>Journal of Chemical Theory and Computation</u> **2025**, <u>21</u>, 3847–3856, PMID: 40117452.
- (35) Shenvi, N.; Tully, J. C. Nonadiabatic dynamics at metal surfaces: Independent electron surface hopping with phonon and electron thermostats. Faraday Discuss. **2012**, 157, 325–335.
- (36) Zhou, G.; Lu, G.; Prezhdo, O. V. Modeling Auger Processes with Nonadiabatic Molecular Dynamics. Nano Letters **2021**, 21, 756–761.
- (37) Hong, J.; Hertl, N.; Maurer, R. J.; Meng, G.; Jiang, B. Vibrational Excitation in Gas-Surface Collisions of CO with Au(111): A First-Principles Nonadiabatic Dynamics Study. The Journal of Physical Chemistry C **2025**, 129, 2944–2952.
- (38) Gardner, J.; Corken, D.; Janke, S. M.; Habershon, S.; Maurer, R. J. Efficient implementation and performance analysis of the independent electron surface hopping method for dynamics at metal surfaces. The Journal of Chemical Physics **2023**, 158.
- (39) Dou, W.; Subotnik, J. E. A many-body states picture of electronic friction: The case of multiple orbitals and multiple electronic states. <u>The Journal of Chemical Physics</u> **2016**, <u>145</u>, 054102.
- (40) Dou, W.; Subotnik, J. E. A Generalized Surface Hopping Algorithm To Model Nonadia-

- batic Dynamics near Metal Surfaces: The Case of Multiple Electronic Orbitals. <u>Journal of</u> Chemical Theory and Computation **2017**, 13, 2430–2439, PMID: 28467702.
- (41) Kapral, R.; Ciccotti, G. Mixed quantum-classical dynamics. <u>The Journal of Chemical Physics</u> **1999**, 110, 8919–8929.
- (42) Galperin, M.; Nitzan, A. Nuclear Dynamics at Molecule–Metal Interfaces: A Pseudoparticle Perspective. <u>The Journal of Physical Chemistry Letters</u> **2015**, <u>6</u>, 4898–4903, PMID: 26589690.
- (43) Tully, J. C. Molecular dynamics with electronic transitions. <u>The Journal of Chemical Physics</u> **1990**, 93, 1061–1071.
- (44) Dou, W.; Nitzan, A.; Subotnik, J. E. Surface hopping with a manifold of electronic states. II. Application to the many-body Anderson-Holstein model. <u>The Journal of Chemical Physics</u> **2015**, 142, 084110.
- (45) Ouyang, W.; Dou, W.; Jain, A.; Subotnik, J. E. Dynamics of Barrier Crossings for the Generalized Anderson–Holstein Model: Beyond Electronic Friction and Conventional Surface Hopping. <u>Journal of Chemical Theory and Computation</u> **2016**, <u>12</u>, 4178–4183, PMID: 27564005.
- (46) Pradhan, C. S.; Jain, A. Detailed Balance and Independent Electron Surface-Hopping Method: The Importance of Decoherence and Correct Calculation of Diabatic Populations. Journal of Chemical Theory and Computation 2022, 18, 4615–4626, PMID: 35880817.
- (47) Tanimura, Y.; Kubo, R. Time Evolution of a Quantum System in Contact with a Nearly Gaussian-Markoffian Noise Bath. <u>Journal of the Physical Society of Japan</u> **1989**, <u>58</u>, 101–114.
- (48) Sun, L.; Hase, W. L. Comparisons of classical and Wigner sampling of transition state energy

- levels for quasiclassical trajectory chemical dynamics simulations. <u>The Journal of Chemical</u> Physics **2010**, 133.
- (49) Huang, Y.-T.; Kuo, P.-C.; Lambert, N.; Cirio, M.; Cross, S.; Yang, S.-L.; Nori, F.; Chen, Y.-N. An efficient Julia framework for hierarchical equations of motion in open quantum systems. Communications Physics **2023**, 6, 313.
- (50) Mercurio, A.; Huang, Y.-T.; Cai, L.-X.; Chen, Y.-N.; Savona, V.; Nori, F. QuantumToolbox.jl: An efficient Julia framework for simulating open quantum systems. <u>arXiv preprint</u> arXiv:2504.21440 **2025**,

# **TOC Graphic**

